Computational and Mathematical Models of the JAK-STAT Signal Transduction Pathway

Vishakha Sharma and Adriana Compagnoni
Stevens Institute of Technology, NJ
Department of Computer Science vsharma1@stevens.edu Adriana.Compagnoni@stevens.edu

Abstract

The JAK (Janus kinase)-STAT (Signal transducer and activator of transcription) signal transduction pathway is a cascade of downstream cellular events initiated from outside of the cell through the cell surface to the DNA in the nucleus, causing transcription. The conventional modeling approach for signal transduction pathways involves solving ordinary differential equations (ODEs). We study here a computational alternative. We build two models of 46 reactions in the JAK-STAT pathway and compare the results. We implement a deterministic mathematical model using the ODEs solver COPASI, and we build a stochastic computational model using the Stochastic Pi Machine (SPiM).

Since dysregulation in the functionality of JAK-STAT pathway results in immune deficiency syndrome and cancers, like lymphomas, leukemia and breast cancer, we believe that models like this have the potential to contribute to cancer research.

Keywords: Stochastic Pi-Calculus, Computational Modeling, Process Algebra, JAK-STAT Signal Transduction Pathway

1. INTRODUCTION

Over the past decade significant progress has been made in the area of modeling for better understanding of the biological behavior of the cell signaling pathways [6, 40, 12, 15]. The conventional mathematical modeling approach involves ordinary differential equations [42, 19, 41]. An alternative modern approach has been proposed that considers each cell as a computing agent. Constructing biological cell signaling pathways based on this approach is known as "Cells as Computation" [36] and "Executable cell biology" [10], which contributes to the better understanding of the dynamic behavior of the complex pathways and the parameters associated with them. This approach bridges the gap between *in silico* experiments on the computer and *in vitro* experimentation in the wet lab. Also, this approach provides future guidance for experimentation, and hence contributes to computational biological research.

Following the pioneering work of Regev and Shapiro [36], our method is based on process algebra, an algebraic approach used to study the interaction between concurrent processes. Process algebra contributes to computational modeling by explaining how complex species, agents or entities interact through communication channels and exchange information [33]. The Pi-Calculus is a mathematical formalism which represents the interaction of heterogeneous entities, and it is able to describe concurrent behaviors whose network configuration may change during computation. The Stochastic Pi-Calculus is an extension of the Pi-Calculus [24], where stochastic rates are imposed on all processes or species to depict their behavior with more accuracy [32]. The Stochastic Pi Machine (SPiM) is a programming language based on the Stochastic Pi-Calculus, and used to model large biological systems incrementally. SPiM is used to run *in silico* simulations, modeling the number of species over a period of time [28].

In this paper, we focus on COPASI [18] and SPiM [28] to compare deterministic and stochastic results, respectively. For instance, a bidirectional reaction, such as Receptor R and Ligand L binding to form the Receptor Ligand complex RL, where k_1 is the rate constant for forward reaction and k_{-1} is the rate constant for reverse reaction, can be written as:

$$\mathrm{R} + \mathrm{L} \underset{k_{-1}}{\overset{k_1}{\longleftrightarrow}} \mathrm{RL}$$

ODEs for the above reaction will be:

i. $d[R]/dt = -k_1[\mathrm{R}][\mathrm{L}] + k_{-1}[\mathrm{RL}]$

ii. $d[L]/dt = -k_1[\mathrm{R}][\mathrm{L}] + k_{-1}[\mathrm{RL}]$

iii. $d[RL]/dt = k_1[\mathrm{R}][\mathrm{L}] - k_{-1}[\mathrm{RL}]$

SPiM agents for the above reaction are (See Section 6.):

```
new rl@k1:chan
let R()=!rl;()
let L() = ?rl;RL()
and RL () = delay@k-1; (R() | L ())
```

The JAK-STAT signaling pathway, an intracellular signaling pathway that leads from cell surface cytokine receptors, provides the fastest track to the nucleus causing alteration in gene transcription [1]. The JAK activation is responsible for cell differentiation, proliferation, cell migration and apoptosis. The cascade of cellular events involved in the JAK-STAT signaling pathway are critical to immune development, hematopoiesis, mammary gland development and lactation,

adipogenesis and sexually dimorphic growth. The gene disruption and mutations activate or fail to regulate the JAK signaling cascade causing inflammatory diseases [27] like diabetic nephropathy [23], tuberculosis [31, 30], erythrocytosis and gigantism, immune deficiency syndrome and cancers, such as leukemia [35], myelofibrosis [8, 13, 39, 14, 38, 26] and breast cancer [16]. Therefore, computational models of the JAK-STAT signal transduction pathway have the potential to contribute to biomedical research.

2. RELATED WORK

The process algebra approach is part of agent-based modeling and simulation (ABMS) [22], which consists of autonomous agents. The interaction and behavior of the agents are described by decision making rules. C-Immsim [34, 4] and PathSim visualizer [29] are based on cellular automata or agent based modeling. The syntax for C-Immsim is similar to an imperative language. It is specifically build to model immune systems. In PathSim visualizer, users can interact with the simulations and use Information-Rich Virtual Environments (IRVEs) to display the results of biological simulations.

Currently, available tools used for modeling cellular signal transduction pathways include Bio-PEPA [7], Cellucidate [9] and Petri Nets [5]. A recent survey study has been performed for the "Activation Cycle of G-proteins by G-protein-coupled Receptors" using these different formalisms based on process calculi [2], but had only 6 reactions. Bio-PEPA is a reaction based formalism where reactants and products are described separately. Cellucidate is a rule-based formalism used to directly model the reactions. Both these formalisms represent species as opposed to individuals. In contrast, SPiM is an individual based formalism that considers each individual as a biological entity and observes its behavior over time. Petri Nets are graphical models of entities that can be used to represent biological components.

The current state of the art lies in genome-scale computational modeling. Recently, a computational model of a small bacterium, *Mycoplasma genitalium*, with only 525 genes, has been built [20].

3. MODEL DESCRIPTION

In earlier studies, ODEs were used to model the control mechanism of the JAK-STAT signal transduction pathway [41]. In our work, we use the Stochastic Pi-Calculus to build the computational model for the JAK-STAT signal transduction pathway.

Figure 1 depicts the 46 reactions of the JAK-STAT signal transduction pathway. Figure 2 zooms into steps ① through ⑮. These steps explain Receptor-JAK binding; Interferon-Receptor binding; IFN-Receptor complex dimerization; IFN-Receptor complex activation; activated IFNRJ2-STAT1c

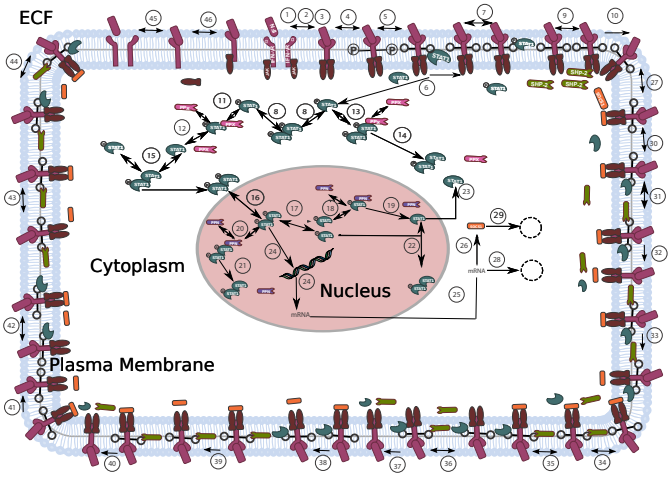

Figure 1. Activation of JAK-STAT signal transduction pathway by cytokine, IFN-γ

binding; STAT1c activation; activated IFNRJ2-STAT1c binding; activated STAT1c dimerization; SHP2 binding; IFNRJ2 dephosphorylation; phosphorylated STAT1c-PPX binding; STAT1c dephosphorylation; PPX binding; STAT1c dimmer phosphorylation; and STAT1c-phosphorylated STAT1c binding, respectively.

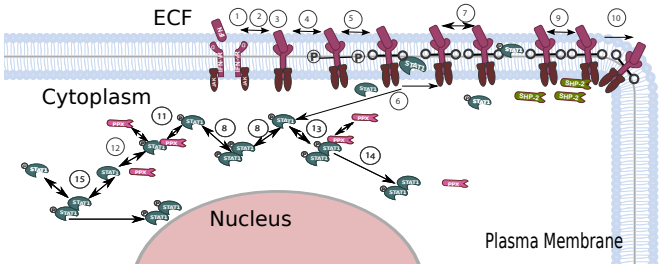

Figure 2. Activation of JAK-STAT signal transduction pathway by cytokine, IFN-γ. Steps ① - ⑮

Figure 3 depicts the formation of R-JAK complex in two different ways. Steps ① through ③ depict Receptor-JAK binding and Interferon-Receptor binding, respectively. Steps ㊺ and ㊻ depict Interferon-Receptor binding and IFNR-JAK binding .

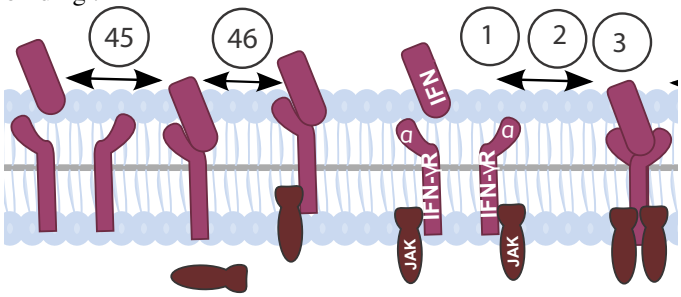

Figure 3. Formation of IFN-γ Receptor in 2 different ways: Steps ㊺ - ㊻ and Steps ① - ③

Figure 4 zooms into steps ⑯ through ㉖, steps ㉘ and ㉙.

These steps explain STAT1c-nuclear transport; phosphorylated STAT1n dimerization; PPN binding; STAT1n dephosphorylation; PPN binding; STAT1n-phosphorylated STAT1n dimerization; STAT1n-phosphorylated STAT1n dimerization; STAT1n transport to cytoplasm; transcription; mRNA transport to cytoplasm; SOCS1 synthesis; mRNAc degradation; and SOCS1 degradation, respectively.

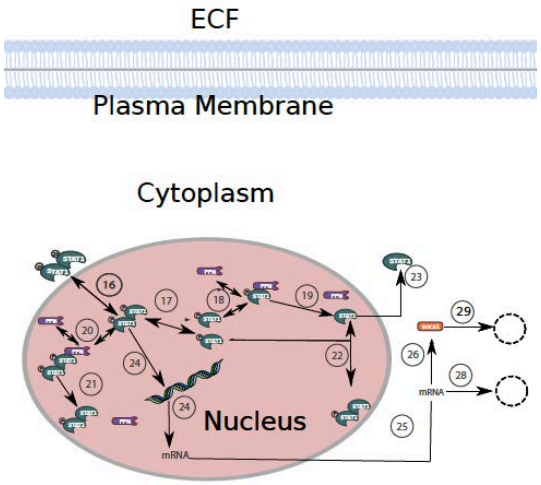

Figure 4. Activation of JAK-STAT signal transduction pathway by cytokine, IFN-γ. Steps ⑯ - ㉖, ㉘ and ㉙

For details on the remaining reactions, see the companion technical report [37].

4. CHEMICAL REACTIONS AND THEIR PARAMETER VALUES

The reactions used to model the JAK-STAT signal transduction pathway and the corresponding rate constants (rate parameters) for each reaction are listed in Table 1. The Michaelis-Menten constant is in nM (Nanomolar). The association reaction rate constants and dissociation reaction rate constants are represented as k and kd, respectively. The first order and second order rate constants are expressed in units of $second^{-1}$ and $nM^{-1}second^{-1}$ [41].

Table 1. Reactions and Rate Parameters [41].

No.	Reactions and Rate Parameters
1	[R] + [JAK] ($k_{01} = 0.1$) $\longleftrightarrow$ ($kd_{01} = 0.05$) [RJ]
2	[RJ] + [IFN] ($k_{02} = 0.02$) $\longleftrightarrow$ ($kd_{02} = 0.02$) [IFNRJ]
3	2[IFNRJ] ($k_{03} = 0.04$) $\longleftrightarrow$ ($kd_{03} = 0.2$) [IFNRJ2]
4	[IFNRJ2] ($k_{04} = 0.005$) $\longrightarrow$ [IFNRJ2*]
5	[IFNRJ2*] + [STAT1c] ($k_{05} = 0.008$) $\longleftrightarrow$ ($kd_{05} = 0.8$) [IFNRJ2*-STAT1c]
6	[IFNRJ2*-STAT1c] ($k_{06} = 0.4$) $\longrightarrow$ [IFNRJ2*] +[STAT1c*]
7	[IFNRJ2*] +[STAT1c*] ($k_{07} = 0.005$) $\longleftrightarrow$ ($kd_{07} = 0.5$) [IFNRJ2*-STAT1c*]
8	2[STAT1c*] ($k_{08} = 0.02$) $\longleftrightarrow$ ($kd_{08} = 0.1$) [STAT1c*-STAT1c*]
9	[IFNRJ2*] + [SHP2] ($k_{09} = 0.001$) $\longleftrightarrow$ ($kd_{09} = 0.2$) [IFNRJ2*-SHP2]
10	[IFNRJ2*-SHP2] ($k_{10} = 0.003$) $\longrightarrow$ [IFNRJ2] + [SHP2]
11	[PPX] + [STAT1c*] ($k_{11} = 0.001$) $\longleftrightarrow$ ($kd_{11} = 0.2$) [PPX-STAT1c*]
12	[PPX-STAT1c*] ($k_{12} = 0.003$) $\longrightarrow$ [PPX] + [STAT1c]
13	[PPX] + [STAT1c*-STAT1c*] ($k_{13} = 0.001$) $\longleftrightarrow$ ($kd_{13} = 0.2$) [PPX-STAT1c*-STAT1c*]
14	[PPX-STAT1c*-STAT1c*] ($k_{14} = 0.003$) $\longrightarrow$ [PPX] + [STAT1c-STAT1c*]
15	[STAT1c] + [STAT1c*] ($k_{15} = 2.0e^{-7}$) $\longleftrightarrow$ ($kd_{15} = 0.2$) [STAT1c-STAT1c*]
16	[STAT1c*-STAT1c*] ($k_{16} = 0.005$) $\longrightarrow$ [STAT1n*-STAT1n*]
17	2[STAT1n*] ($k_{17} = 0.02$) $\longleftrightarrow$ ($kd_{17} = 0.1$) [STAT1n*-STAT1n*]
18	[PPN] + [STAT1n*] ($k_{18} = 0.005$) $\longrightarrow$ [PPN-STAT1n*]
19	[PPN-STAT1n*] ($k_{19} = 0.005$) $\longrightarrow$ [PPN] + [STAT1n]
20	[PPN] + [STAT1n*-STAT1n*] ($k_{20} = 0.001$) $\longleftrightarrow$ ($kd_{20} = 0.2$) [PPN-STAT1n*-STAT1n*]
21	[PPN-STAT1n*-STAT1n*] ($k_{21} = 0.005$) $\longrightarrow$ [PPN] + [STAT1n-STAT1n*]
22	[STAT1n] + [STAT1n*] ($k_{22} = 2.0e^{-7}0$) $\longleftrightarrow$ ($kd_{22} = 0.2$) [STAT1n-STAT1n*]
23	[STAT1n] ($k_{23} = 0.05$) $\longrightarrow$ [STAT1c]
24	V_{max}[STAT1n*-STAT1n*]/(K_M+[STAT1n*-STAT1n*]); ($V_{max} = 0.01$, $K_M = 400$)
25	[mRNAn] ($k_{25} = 0.001$) $\longrightarrow$ [mRNAc]
26	[mRNAc] ($k_{26} = 0.01$) $\rightarrow$ [SOCS1]
27	[IFNRJ2*] + [SOCS1] ($k_{27} = 0.02$) $\longleftrightarrow$ ($kd_{27} = 0.1$) [IFNRJ2*-SOCS1]
28	[mRNAc] ($k_{28} = 5.0e^{-4}$) $\longrightarrow$;
29	[SOCS1] ($k_{29} = 5.0e^{-4}$) $\longrightarrow$;
30	[IFNRJ2*-SOCS1] + [STAT1c] ($k_{30} = 0.008$) $\longleftrightarrow$ ($kd_{30} = 0.8$) [IFNRJ2*-SOCS1-STAT1c]
31	[IFNRJ2*-SOCS1-STAT1c] + [SHP2] ($k_{31} = 0.001$) $\longleftrightarrow$ ($kd_{31} = 0.2$)[IFNRJ2*-SHP2-SOCS1-STAT1c]
32	[IFNRJ2*-SHP2-SOCS1-STAT1c] ($k_{32} = 0.003$) $\rightarrow$ [IFNRJ2] + [SHP2] + [SOCS1] + [STAT1c]
33	[IFNRJ2*-SHP2-SOCS1-STAT1c] ($k_{33} = 5.0e^{-4}$) $\rightarrow$ [IFNRJ2*-SHP2-STAT1c]
34	[IFNRJ2*-SOCS1] + [SHP2] ($k_{34} = 0.001$) $\longleftrightarrow$ ($kd_{34} = 0.2$) [IFNRJ2*-SHP2-SOCS1]
35	[IFNRJ2*-SHP2-SOCS1] + [STAT1c] ($k_{35} = 0.008$) $\longleftrightarrow$ ($kd_{35} = 0.8$) [IFNRJ2*-SHP2-SOCS1-STAT1c]
36	IFNRJ2*-STAT1c] + [SHP2] ($k_{36} = 0.001$) $\longleftrightarrow$ ($kd_{36} = 0.02$) [IFNRJ2*-SHP2-STAT1c]
37	[IFNRJ2*-SHP2-STAT1c] ($k_{37} = 0.003$) $\longrightarrow$ [STAT1c] + [SHP2] + [IFNRJ2]
38	[IFNRJ2*-SOCS1-STAT1c] ($k_{38} = 5.0e^{-4}$) $\longrightarrow$ [IFNRJ2*-STAT1c]
39	[IFNRJ2*-SHP2-SOCS1] ($k_{39} = 5.0e^{-4}$) $\longrightarrow$ [IFNRJ2*-SHP2]
40	[IFNRJ2*-SHP2-SOCS1] ($k_{40} = 0.003$) $\longrightarrow$ [IFNRJ2] + [SHP2] + [SOCS1]
41	[IFNRJ2*-SOCS1] ($k_{41} = 5.0e^{-4}$) $\longrightarrow$ [IFNRJ2*]
42	[IFNRJ2*-STAT1c] + [SOCS1] ($k_{42} = 0.02$) $\longleftrightarrow$ ($kd_{42} = 0.1$) [IFNRJ2*-SOCS1-STAT1c]
43	[IFNRJ2*-SHP2] + [SOCS1] ($k_{43} = 0.02$) $\longleftrightarrow$ ($kd_{43} = 0.1$) [IFNRJ2*-SHP2-SOCS1]
44	[IFNRJ2*-SHP2-STAT1c] + [SOCS1] ($k_{44} = 0.02$) $\longleftrightarrow$ ($kd_{44} = 0.1$) [IFNRJ2*-SHP2-SOCS1-STAT1c]
45	[IFN] + [R] ($k_{45} = 0.02$) $\longleftrightarrow$ ($kd_{45} = 0.02$) [IFNR]
46	[IFNR] + [JAK] ($k_{46} = 0.1$) $\longleftrightarrow$ ($kd_{46} = 0.05$) [IFNRJ]

5. REACTION KINETICS

Most of the biochemical reactions that occur in the cell are catalyzed by enzymes. The enzyme E reacts with substrate S to yield Enzyme-Substrate complex ES which in turn yields product P. This equation can be represented as:

$$\mathrm{E} + \mathrm{S} \underset{k_{-1}}{\overset{k_1}{\longleftrightarrow}} \mathrm{ES} \xrightarrow{k_2} \mathrm{P} + \mathrm{E}$$

where, k_1, k_{-1} and k_2 are rate constants. The double arrow ($\leftrightarrow$) means that the reaction is reversible, and the single arrow ($\rightarrow$) means that reaction can occur in one direction.

Law of Mass Action. As per the Law of Mass Action, the rate of a reaction is proportional to the product of the concentration of the reactants. Assuming, the concentration of reactants as s=[S], e=[E], c=[ES] and p=[P], where [ ] means concentration. By the Law of Mass Action, we derive one nonlinear ordinary differential equation for each reactant, which are as follows:

i. $d[S]/dt = -k_1[\mathrm{E}][\mathrm{S}] + k_{-1}[\mathrm{ES}]$

ii. $d[E]/dt = -k_1[\mathrm{E}][\mathrm{S}] + (k_{-1} + k_2)[\mathrm{ES}]$

iii. $d[ES]/dt = k_1[\mathrm{E}][\mathrm{S}] - (k_{-1} + k_2)[\mathrm{ES}]$

iv. $d[P]/dt = k_2[\mathrm{ES}]$

Michaelis-Menten. As per the Michaelis-Menten kinetics, the formation of the complex c, [ES] is very fast, and the substrate s is in a chemical equilibrium with the complex c, [ES] which implies:

$$[\mathrm{ES}](t) = [ES]_0[S](t)/([S](t) + K_M), \text{ and}$$
$$K_M = (k_{-1} + k_2)/k_1$$

We consider the initial conditions as [S](0) = $[S]_0$, [E](0) = $[E]_0$, [ES](0) = 0 and [P](0) =0 to yield product P from substrate S.

$$d[S]/dt = -k_2[E]_0[S]/([\mathrm{S}] + K_M)$$

K_M is known as the Michaelis constant, that is the substrate concentration at which the reaction rate is half of V_{max}, and $k_2[E]_0$ is the V_{max}, which is the maximum reaction velocity at maximum substrate concentration. The substrate concentration does not change during the initial transient stage, because the enzyme is always present in small quantities compared to the substrate. Hence, [S] = $[S]_0$. This is known as pseudo-or quasi-steady state approximation [25]. Since, the initial concentration of the substrate is very small compared to the value of K_M the transcription rate is directly proportional to the substrate concentration.

$$\text{transcription rate} \sim= -V_{max}/K_M$$

The rate constant k = V_{max}/K_M is a measure of how efficiently a substrate is converted into a product by an enzyme.

Translation of Michaelis-Menten kinetics to Law of Mass Action in SPiM. In SPiM, the simulator understands the reactions written in Law of Mass Action kinetics. To model any reaction which is in Michaelis-Menten kinetics, we need to first translate it into Law of Mass Action kinetics. In the Yamada model, all the reactions are based on the Law of Mass Action kinetics, except for reaction 24, which is based on Michaelis-Menten kinetics. In reaction 24, STAT1n*-STAT1n*, which are the phosphorylated STAT1 dimers in the nucleus reproduce mRNA as a result of transcription. The process of transcription is an enzymatic reaction and hence based on Michaelis-Menten kinetics. The ODE is:

$$\mathrm{d[P]/dt} = V_{max}[\text{STAT1n*-STAT1n*}]/(K_M + [\text{STAT1n*-STAT1n*}])$$

The equivalent SPiM code for the above reaction in ODEs can be written as:

```
STAT1nLSTAT1nL() = delay@r24; (STAT1nLSTAT1nL()
                              |mRNAn())
```

We use the quasi-steady state approximation to calculate the value of r24 or k24 as 2.5e-5 to model this equation where r24 or k24 is the rate constant for transcription. The maximum reaction velocity V_{max} is 0.01, and Michaelis-Menten constant K_M is 400. The substrate in this reaction is STAT1n*-STAT1n*, and the product is mRNAn (or mRNA in nucleus).

6. COMPUTATIONAL MODELING IN STOCHASTIC PI-CALCULUS

The Stochastic Pi-Calculus can be used to model the behavior of biological systems in a natural way. In any biological pathway, any protein can be described as a process P, and the changes in the state of P, such as phosphorylation can be described using a send/receive handshake between P and a kinase. Spontaneous changes, such as first order reactions can be represented with a delay action. Both send/receive handshake and delay reactions have associated reaction rates, which in this modeling method represent kinetic rates [32]. The SPiM simulator is based on Gillespie's algorithm, that determines the probability of the reaction to be executed next, based on the concentration of the reactants and the reaction rate associated with that reaction [11].

Consider the reaction 45, Interferon-Receptor Binding in Table 1.

$$[\mathrm{IFN}] + [\mathrm{R}] \leftrightarrow [\mathrm{IFNR}];\ k_{45} = 0.02\ ,\ kd_{45} = 0.02$$

In process algebra, binding of two proteins can be explained as the communication between two proteins via a communication channel. In the above example, R (Receptor) and IFN (Interferon) interact to form the complex IFNR (Interferon-Receptor complex) via channel c45 as shown in Table 2. The standard notation !c45 is used to send a message over channel c45, and symmetrically ?c45 is used to receive a message over

the channel c45. The statement `new c45@r45:chan` declares a new channel c45 for communication between the two proteins R and IFN at a rate r45 to form the complex IFNR. The statement `IFNR() = delay@s45; (R()|IFN())` declares a first order reaction at a reaction rate s45 for the dissociation of the complex IFNR into R and IFN. The rate constants k45, kd45 and s45 are the association, dissociation and delay rate constants respectively, as shown in Table 2. The initial concentrations of Receptor and Interferon are 100nM as per the Yamada, et. al model [41]. The reaction volume is assumed to be 1 Litre (Molar = molecules per Litre, molecules = 6.022×10^{23} (Avogadro's Constant) and 1nM = 10^{-9}M). Figure 5 shows the process model generated by the SPiM code in Table 2. The equivalent code for the same equation in COPASI is shown in Table 3. Figure 6 shows the simulation results produced by SPiM.

```
directive sample 28.8e+3 1000
directive plot R();IFN();IFNR()
directive graph
val k45 = 0.02
val kd45 = 0.02
val r45 = k45
val s45 = kd45
new c45@r45:chan

let R() = !c45; ()
and IFN() = ?c45; IFNR()
and IFNR() = delay@s45; (R()|IFN())

run 100 of (R() | IFN())
```

Table 2. SPiM code for reaction 45 (Interferon-Receptor Binding).

Table 3. COPASI code for reaction 45 (Interferon-Receptor Binding).

No. Name	Equation	Rate Law
45 Interferon-Receptor Binding	R + IFN ↔ IFNR	Mass Action (reversible)

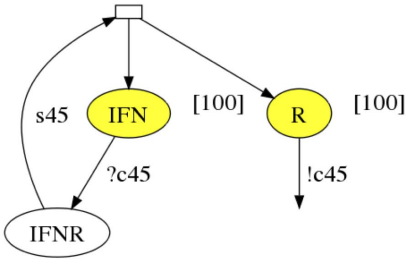

Figure 5. Process model generated by SPiM for the reaction 45 (Interferon-Receptor Binding).

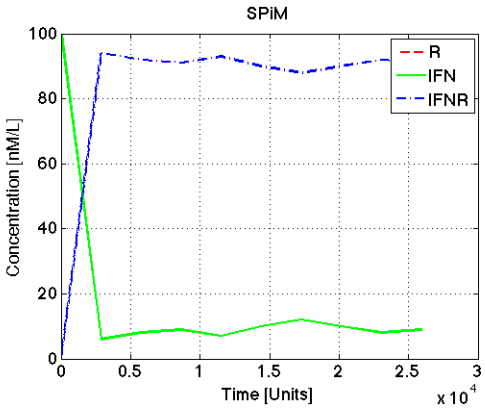

Figure 6. Simulation result produced using SPiM for binding of two proteins, Receptor, R (red) and Interferon, IFN (green) to form protein complex, IFNR (blue).

7. RESULTS

In this study we have used COPASI, COmplex PAthway SImulator [18] and SPiM [28] to produce our deterministic and stochastic simulation results. COPASI automatically converts the reaction equations to ODEs using ODEPACK [17].

The "directive plot" statement in the SPiM code declares the species or processes to be plotted during, simulation and the "run" statement initializes the concentration of the species. The reaction rates are translated based on the literature [21]. We have scaled the model to 1:10 because SPiM does not work with very low or very high concentrations. The low numbers may produce incorrect results and very high numbers make the simulation very slow. Hence, scaling is done to operate within these limits. The initial concentration of R is 10; JAK is 10; IFN is 10; STAT1c is 1,000; SHP2 is 100; PPX is 50; and PPN is 60 in the JAK-STAT model of Yamada, et. al [41]. In our model, the initial concentration of R is 100; JAK is 100; IFN is 100; STAT1c is 10,000; SHP2 is 1,000; PPX is 500; and PPN is 600.

The simulation of JAK-STAT signal transduction model was run over 28,800 time units, which is equivalent to 8 hours of real time, with 1,000 sampling events over this time range. The states generated by SPiM are the protein complexes and are considered as unique species.

We implemented the model of Yamada, et. al [41] both in COPASI and SPiM, and we obtained consistent results. Figure 7 and Figure 8 show the simulation results produced using COPASI and SPiM, respectively.

Signal Transducer and Activator of Transcription in cytoplasm (STAT1c). The initial concentration of STAT1c under steady state is 1000nM/L as shown in the SPiM simulation result produced in Figure 8. Due to the interferon signaling, the STAT1c is phosphorylated in the cytoplasm. The phosphorylated STAT1c is transported to the nucleus causing an increase in the STAT1n and thus resulting a decrease in the concentration of STAT1c in the cytoplasm. In the nucleus, the

STAT1n are phosphorylated as well as dephosphorylated. The phosphorylated STAT1n activates transcription, which leads to the synthesis of SOCS1. The dephosphorylated STAT1n are transported to the cytoplasm and cause an increase in the concentration of STAT1c, which is evident from the graph.

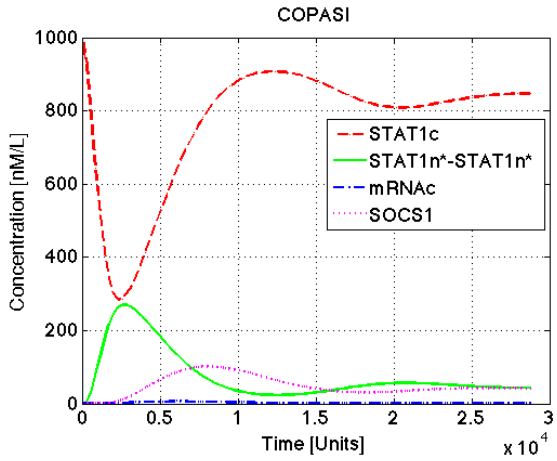

Figure 7. Simulation results of deterministic ODEs model in COPASI [18]. Population of mRNAc (blue), STAT1c (red), SOCS1 (magenta) and STAT1n*-STAT1n* (green).

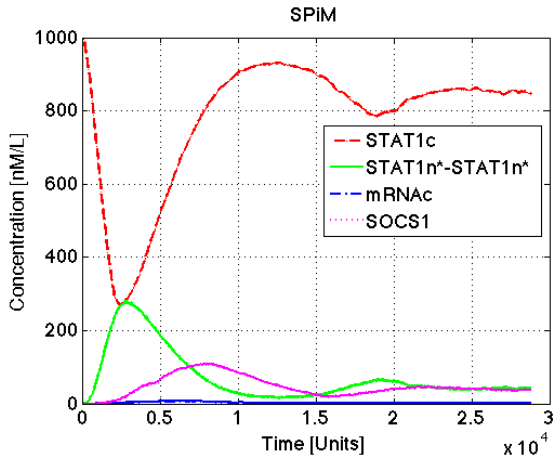

Figure 8. Simulation results of non-deterministic stochastic model in SPiM [28]. Population of mRNAc (blue), STAT1c (red), SOCS1 (magenta) and STAT1n*-STAT1n* (green).

Phosphorylated dimers of STAT1 in nucleus (STAT1n*-STAT1n*). The SPiM simulation result for STAT1n*-STAT1n* shown in Figure 8 shows the peak concentration of STAT1n*-STAT1n* as 270-275nM/L. The phosphorylated dimers of STAT1 increase in the nucleus due to the JAK signaling. The inhibition caused by SOCS1 in kinase activity is responsible for the decline in the plot for STAT1n*-STAT1n* concentration.

mRNA in cytoplasm (mRNAc). Figure 8 depicts the simulation results of the interferon gamma signaling through the JAK-STAT pathway. The output for this pathway is mRNA, produced during transcription. The peak level of the concentration of mRNA is 6nM/L, an interferon-dependent gene. The mRNAc stands for the mRNA transported from nucleus to the cytoplasm. These mRNA are responsible for the synthesis of SOCS1 gene.

Suppressor of cytokine signaling-1 (SOCS1). From the SPIM simulation result for SOCS1 depicted in Figure 8, it is evident that SOCS1 inhibits the JAK signaling in the cells. The first peak in the plot shows the protein synthesis due to JAK signaling. The peak concentration of the SOCS1 in the plot is 100nM/L. The decline in the plot after the first peak is due to the negative feedback caused by the synthesis of SOCS1 on the kinase activity. The second peak is not the real signal, but the echo of the signal.

Simulation results of mRNA in cytoplasm (mRNAc) in COPASI and SPiM. Figure 9 depicts the simulation results produced in COPASI, and two runs using SPiM for the mRNA in the cytoplasm (mRNAc). In the plot, the x-axis is the simulation time in seconds, and y-axis is the concentration of proteins in nM/L. The red color plot is the result produced from COPASI. The green color plot is the result produced by SPiM during first run. The blue color plot is the result produced using SPiM during 2nd run. The variations in the results produced using SPiM shows its stochastic nature.

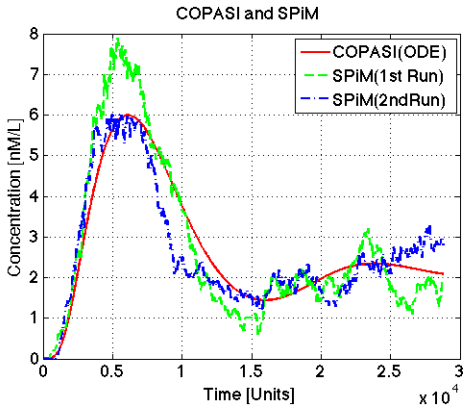

Figure 9. Simulation result for the population of mRNA in the cytoplasm mRNAc, using COPASI (red) and SPIM (green and blue).

8. CONCLUSION

Biologists have developed a rich body of knowledge on signal transduction pathways in cells. However, for the most part, such information is static, mostly recorded in scholarly publications or stored in centralized repositories, where integration of such fragmented knowledge remains a challenging task, and where analyzing the consequences of pathways perturbations and cross talk is a daunting job. This reality mo-

tivates the need for modular executable computational models as platforms to explore the effects of hypothetical drugs. We build a computational model for 46 reactions, JAK-STAT signal transduction pathway. JAK-STAT signal transduction pathway is the fastest track to the nucleus with potential contributions to cancer research, and in particular in the study of the causes of gene alteration.

Computational models have become an essential tool in engineering and science. Using computational methods, we can develop models parameterized by different options for proteins, drugs, etc., and compare predictions in a virtual laboratory. These predictions will suggest a narrow space of wet lab experiments significantly cutting down cost and time, making an unattainable goal in the traditional setting possible with our new technology. To summarize, this study can be helpful in understanding the cell signaling pathways, reaction kinetics and two different approaches, namely, ODEs and Stochastic Pi-Calculus to build a computational model. This study can also play an important role in building a genome-scale computational model of a cell in the future.

We build our model using Stochastic Pi Machine, which is based on the Stochastic Pi-Calculus and is used to build computational models for biological processes. SPiM uses a graphical representation to model small and simple biological systems, such as protein synthesis, and build large and complex systems, like a signal transduction pathways consisting of those smaller biological sub-systems. The Stochastic Pi-Calculus approach is "internal" as it considers the interactions between the processes and the quantitative information, such as reaction rates. On the other hand, ODEs have an "external" approach by considering the temporal evolution of species by modeling the mutual relationships among variables that represent the concentrations of the species involved. The behavioral expressivity of the Stochastic Pi-Calculus out stands the analytical behavior of the ODEs systems [3].

Figure 9 highlights the difference between stochastic (SPiM) and non-stochastic (ODE-COPASI) modeling. The ODE results are an average of all possible outcomes, whereas each SPiM output gives a stochastic variation of the results. While the deterministic results of ODE modeling may suggest the efficacy of a potential drug or inhibitor in an average case, the stochastic variations can expose cases where it would not be effective.

In our computational model, we scale the initial concentrations to accomodate the fact that solving ordinary differential equations is faster than executing a concurrent model. We also explain how the enzyme Michaelis-Menten kinetics is translated into the Law of Mass action, and how the quasi-steady state approximation contributes to reaction rate translation from ODEs to SPiM. Our model can now be used to predict the behavior of the JAK-STAT pathway in the presence of inhibitory agents, creating a platform to assist in the development of new drugs.

9. ACKNOWLEDGEMENT

We are grateful to Luca Cardelli and Andrew Phillips of Microsoft Research for their help with understanding reaction kinetics and their translation into SPiM. We also thank Susanne Wetzel, Philip Leopold, Peter Tolias, Arthur Ritter and Eunhee Kang of Stevens Institute of Technology for their suggestions during the modeling work.

REFERENCES

[1] Bruce Alberts, Alexander Johnson, Julian Lewis, Martin Raff, Keith Roberts, Peter, and Peter Walter. *Molecular Biology of the Cell*. Garland Science, 2008.

[2] Yifei Bao, Adriana B. Compagnoni, Joseph Glavy, and Tommy White. Computational modeling for the activation cycle of G-proteins by G-protein-coupled receptors. In *MeCBIC*, pages 39–53, 2010.

[3] Luca Bortolussi and Alberto Policriti. Connecting process algebras and differential equations for systems biology. In *6th Workshop on Process Algebras and Stochastically Timed Activities (PASTA)*, June 2006.

[4] Filippo Castiglione and Massimo Bernaschi. C-ImmSim: playing with the immune response. In *Proceedings of the Sixteenth International Symposium on Mathematical Theory of Networks and Systems (MTNS)*, 2004.

[5] Claudine Chaouiya. Petri net modelling of biological networks. *Briefings in Bioinformatics*, 8(4):210–219, 2007.

[6] Federica Ciocchetta, Adam Duguid, and Maria Luisa Guerriero. A compartmental model of the cAMP/PKA/MAPK pathway in Bio-PEPA. In *MeCBIC*, pages 71–90, 2009.

[7] Federica Ciocchetta and Jane Hillston. Bio-pepa: A framework for the modelling and analysis of biological systems. *Theoretical Computer Science*, 410(33-34):3065–3084, August 2009.

[8] Stefan N. Constantinescu, Michael Girardot, and Christian Pecquet. Mining for JAK-STAT mutations in cancer. *Trends in Biochemical Sciences*, 33(3):122–131, 2008.

[9] Vincent Danos, Jerome Feret, Walter Fontana, and et al. Rule-based modelling of cellular signalling. In *CONCUR 2007. Concurrency Theory*, volume 4703 of *Lecture Notes in Computer Science*, pages 17–41. Springer Berlin / Heidelberg, 2007.

[10] Jasmin Fisher and Thomas A. Henzinger. Executable Cell Biology. *Nature Biotechnology*, 25(11):1239–1249, November 2007.

[11] Daniel T. Gillespie. Exact stochastic simulation of coupled chemical reactions. *The Journal of Physical Chemistry*, 81(25):2340–2361, December 1977.

[12] Maria Luisa Guerriero, Anna Dudka, Nicholas Underhill-Day, and et al. Narrative-based computational modelling of the Gp130/JAK/STAT signalling pathway. *BMC Systems Biology*, 3(1):40, 2009.

[13] C. Harrison, J.J. Kiladjian, H.K. Al-Ali, and et al. Jak inhibition with ruxolitinib versus best available therapy for myelofibrosis. *New Eng. J. Med.*, 366(9):787–98, 2012.

[14] H.C. Hasselbalch. Perspectives on chronic inflammation in essential thrombocythemia, polycythemia vera, and myelofibrosis: is chronic inflammation a trigger and driver of clonal evolution and development of accelerated atherosclerosis and second cancer? *Blood.Epub ahead of print February 7*, 119(14):3219–25, 2012.

[15] Monika Heiner, Ina Koch, and Jurgen Will. Model validation of biological pathways using Petri nets–demonstrated for apoptosis. *Biosystems*, 75(1-3):15–28, 2004.

[16] Hector Hernandez-Vargas, Maria Ouzounova, Florence Le Calvez-Kelm, and et al. Methylome analysis reveals Jak-STAT pathway deregulation in putative breast cancer stem cells. *Epigenetics*, 6(4):428–439, 2011.

[17] A.C. Hindmarsh. Odepack, a systematized collection of ode solvers. *In Stepleman,R.S. (ed.), Scientific Computing*, pages 55–64, 1983.

[18] Stefan Hoops, Sven Sahle, Ralph Gauges, and et al. Copasi - a complex pathway simulator. *Bioinformatics*, 22(24):3067–3074, October 2006.

[19] JJ Hornberg, B Binder, FJ Bruggeman, B Schoeberl, and et al. Control of mapk signalling: from complexity to what really matters. *Oncogene*, 24:5533–5542, 2005.

[20] Jonathan R. Karr, Jayodita C. Sanghvi, Derek N. Macklin, and et al. A Whole-Cell computational model predicts phenotype from genotype. *Cell*, 150(2):389–401, 2012.

[21] Luca and Cardelli. On process rate semantics. *Theor. Comput. Sci.*, 391(3):190–215, 2008.

[22] CM Macal and MJ North. Tutorial on agent-based modelling and simulation. *Journal of Simulation*, 4(3):151–162, 2010.

[23] Mario B. Marrero, Amy K. Banes-Berceli, David M. Stern, and Douglas C. Eaton. Role of the JAK/STAT signaling pathway in diabetic nephropathy. *American Journal of Physiology - Renal Physiology*, 290(4):F762–F768, 2006.

[24] Robin Milner, Joachim Parrow, and David Walker. A calculus of mobile processes, parts i and ii. *Inf. Comput.*, 100(1):1–77, September 1992.

[25] James. D. Murray, editor. *Mathematical Biology. An Introduction*, volume 17 of *Interdisciplinary Applied Mathematics*. Springer, 3rd edition, 2002.

[26] National Institutes of Health. Study of efficacy and safety in polycythemia vera subjects who are resistant to or intolerant of hydroxyurea: JAK Inhibitor JAKAVI (INCB018424) Tablets Versus Best Available Care: The RESPONSE Trial, 2010. Available at.

[27] Damla Olcaydu and Robert Kralovics. The role of janus kinases in hematopoietic malignancies. In Thomas Decker and Mathias Muller, editors, *Jak-Stat Signaling : From Basics to Disease*, pages 239–258. Springer Vienna, 2012.

[28] Andrew Phillips and Luca Cardelli. Efficient, correct simulation of biological processes in the stochastic pi-calculus. In *Computational Methods in Systems Biology*, volume 4695 of *LNCS*, pages 184–199. Springer, September 2007.

[29] Nicholas F. Polys, Doug A. Bowman, Chris North, and et al. Pathsim visualizer: an information-rich virtual environment framework for systems biology. In *Web3D 04: Proceedings of the ninth international conference on 3D Web technology*, pages 7–14, New York, NY, USA, 2004. ACM.

[30] Savita Prabhakar, Yaming Qiao, Antony Canova, and et al. IFN-$\alpha\beta$ secreted during infection is necessary but not sufficient for negative feedback regulation of IFN-$\alpha\beta$ signaling by mycobacterium tuberculosis. *The Journal of Immunology*, 174(2):1003–1012, 2005.

[31] Savita Prabhakar, Yaming Qiao, Yoshihiko Hoshino, and et al. Inhibition of response to alpha interferon by mycobacterium tuberculosis. *Infection and Immunity*, 71(5):2487–2497, 2003.

[32] Corrado Priami. Stochastic pi-calculus. *Comput. J.*, 38(7):578–589, 1995.

[33] Corrado Priami, Aviv Regev, Ehud Y. Shapiro, and William Silverman. Application of a stochastic name-passing calculus to representation and simulation of molecular processes. *Inf. Process. Lett.*, 80(1):25–31, 2001.

[34] Nicolas Rapin, Ole Lund, and Filippo Castiglione. Immune system simulation online. *Bioinformatics*, 2011.

[35] Jason S. Rawlings, Kristin M. Rosler, and Douglas A. Harrison. The JAK/STAT signaling pathway. *Journal of Cell Science*, 117(7):1281–1283, 2004.

[36] Aviv Regev and Ehud Shapiro. Cells as computation. *Nature*, 419:26, 2002.

[37] Vishakha Sharma and Adriana Compagnoni. Computational and mathematical models of the JAK-STAT signal transduction pathway. Technical Report CS-2013-1, Stevens Institute of Technology, 2013.

[38] S. Verstovsek, H. Kantarjian, R.A. Mesa, and et al. Safety and efficacy of JAK1 and JAK2 inhibitor, INCB018424, in myelofibrosis. *New Eng. J. Med.*, 363:1117–1127, 2010.

[39] S. Verstovsek, R.A. Mesa, J. Gotlib, and et al. A double-blind, placebo-controlled trial of ruxolitinib for myelofibrosis. *New Eng. J. Med.*, 366(9):799–807, 2012.

[40] Dennis Wang, Luca Cardelli, Andrew Phillips, Nir Piterman, and Jasmin Fisher. Computational modeling of the EGFR network elucidates control mechanisms regulating signal dynamics. *BMC Systems Biology*, 3(1):118, 2009.

[41] Satoshi Yamada, Satoru Shiono, Akiko Joo, and Akihiko Yoshimura. Control mechanism of JAK/STAT signal transduction pathway. *FEBS Letters*, 534(16):190–196, 2003.

[42] Tau M. Yi, Hiroaki Kitano, and Melvin I. Simon. A quantitative characterization of the yeast heterotrimeric G protein cycle. *Proceedings of the National Academy of Sciences*, 100(19):10764–9, Sep 2003.